GMA 09
Riunione del Gruppo Materiali
dell'AIMETA
Politecnico di Milano
23-24 Gennaio 2009

Approccio micromeccanico alla modellazione di processi fisiologici

Paolo Bisegna

Università di Roma Tor Vergata
Dipartimento di Ingegneria Civile

Towards predictive modeling of biological systems

- Need to cope with different space and time scales:
- nanoscale: macromolecules, biological membranes, citoskeleton, sarcomere (biochemical reaction cascades, cell response and motility, adaptation, etc.)
- microscale: cells and tissues (growth and remodeling, electric conduction, interface with biomedical devices)
- macroscale: organs, systems, whole organisms (overall behavior, signs and symptoms)
- all space scales: highly-regulated time dependent behavior at various time scales (e.g., acute/chronic loadings, early/late response)

Bridging between scales

- Attempts to elucidate macroscopic behaviors based on nanoscopic and microscopic data are valuable
- Fully realistic simulation is impracticable because of the cost entailed and huge amount of data required
- Abstraction and modeling are needed: methods of mechanics of materials turns out to be very useful
- Noteworthy examples in GMA09 presentations. Here:
  - ✓Phototransduction (nanoscale)
  - ✓Bioimpedance measurements (microscale)

Coauthors

M. Amar	University of Rome La Sapienza
D. Andreucci	University of Rome La Sapienza
G. Caruso	ITC – CNR
F. Caselli	University of Rome Tor Vergata
E. DiBenedetto	Vanderbilt University
R. Gianni	University of Rome La Sapienza
H. Hamm	Vanderbilt University

Phototransduction

Transduction of photons into electrical signals

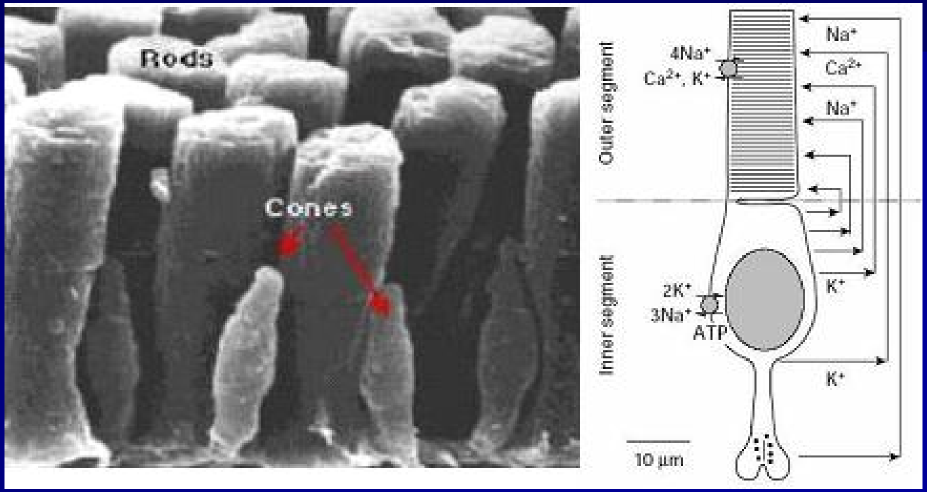

Biochemical process involving diffusion of second messengers into highly structured photoreceptors

Archetypal signaling: similar mechanisms in response to odorant, tastant, some hormones

Modeling phototransduction may help elucidating cell signaling mechanisms and single out drug targets

Retinal organization

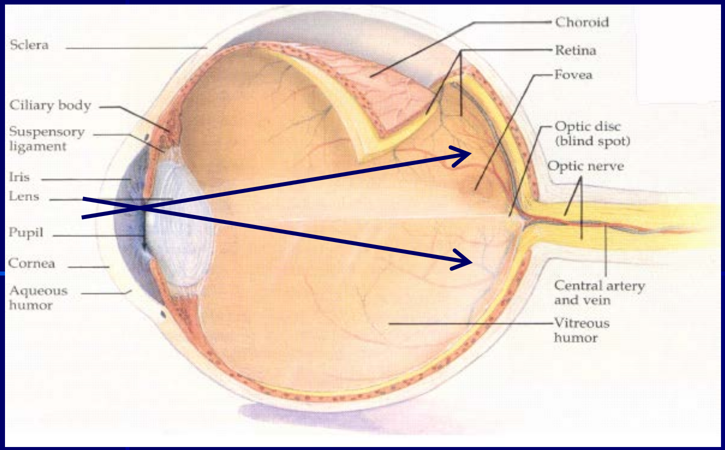

Retinal layers

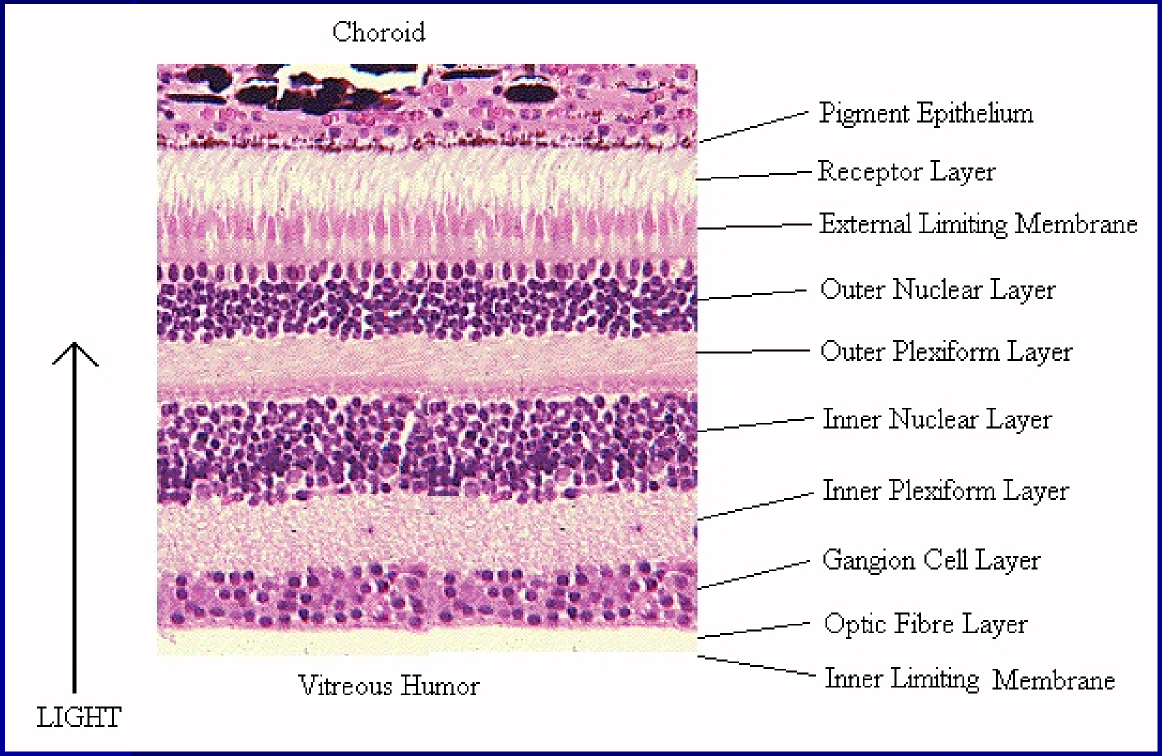

Retinal cell types

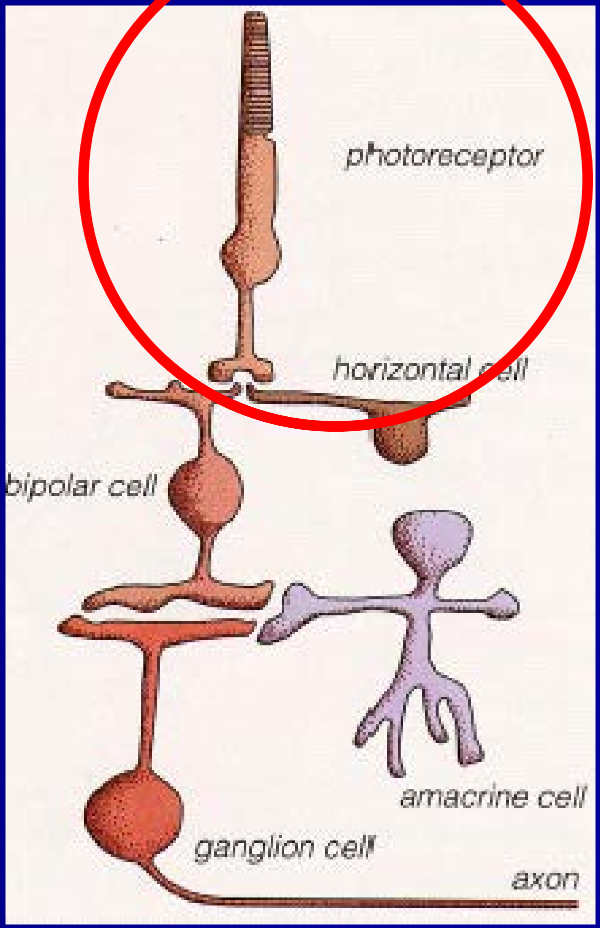

Photoreceptors

Cones:

Photopic vision
Virtually no saturation
Dynamic range : 5 decades

Rods:

Scotopic vision
Single photon sensitivity
Response saturation
at 100 photon flash
Limited dynamic range, 2 decades

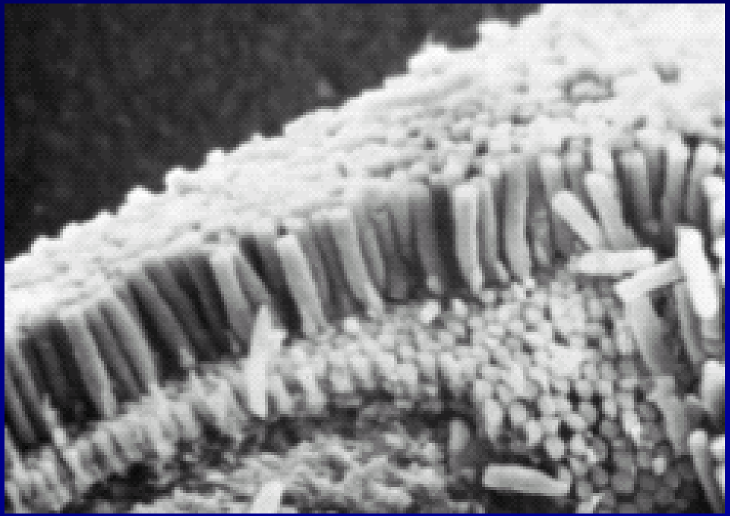

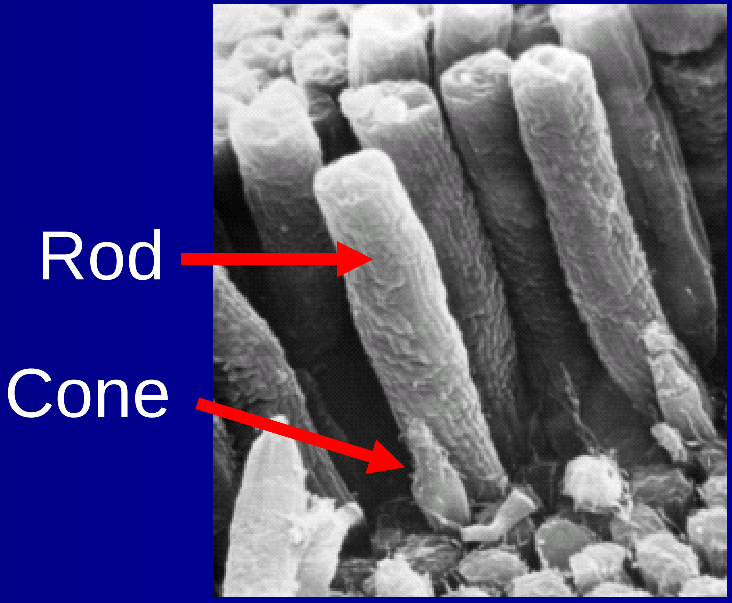

Visible spectrum

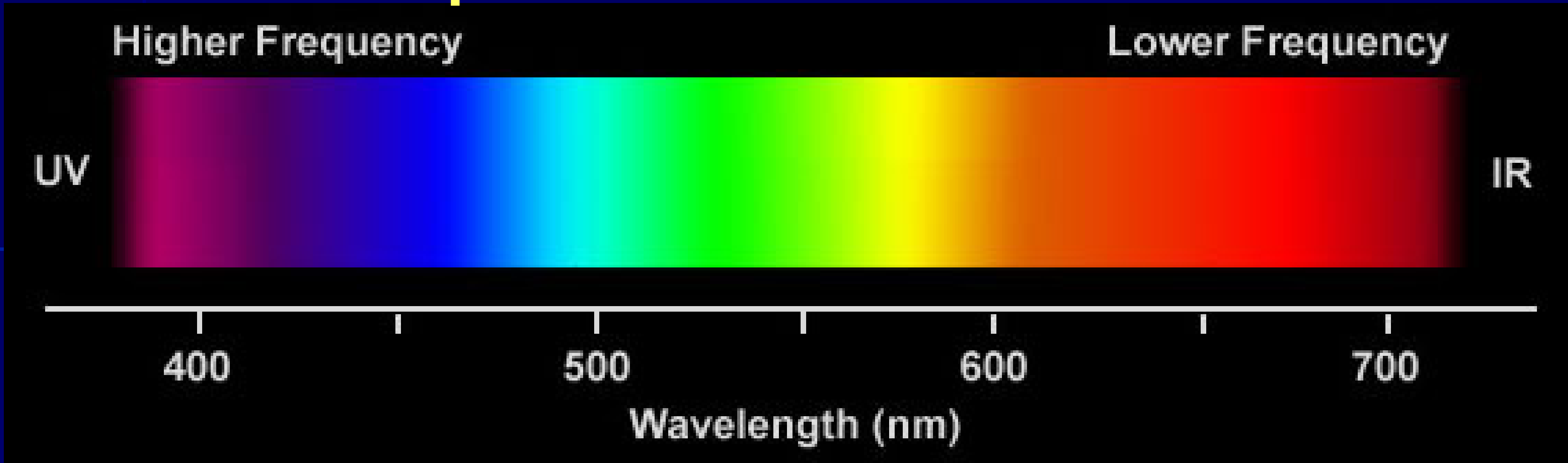

Rods: Cones: blue green red

500 nm max

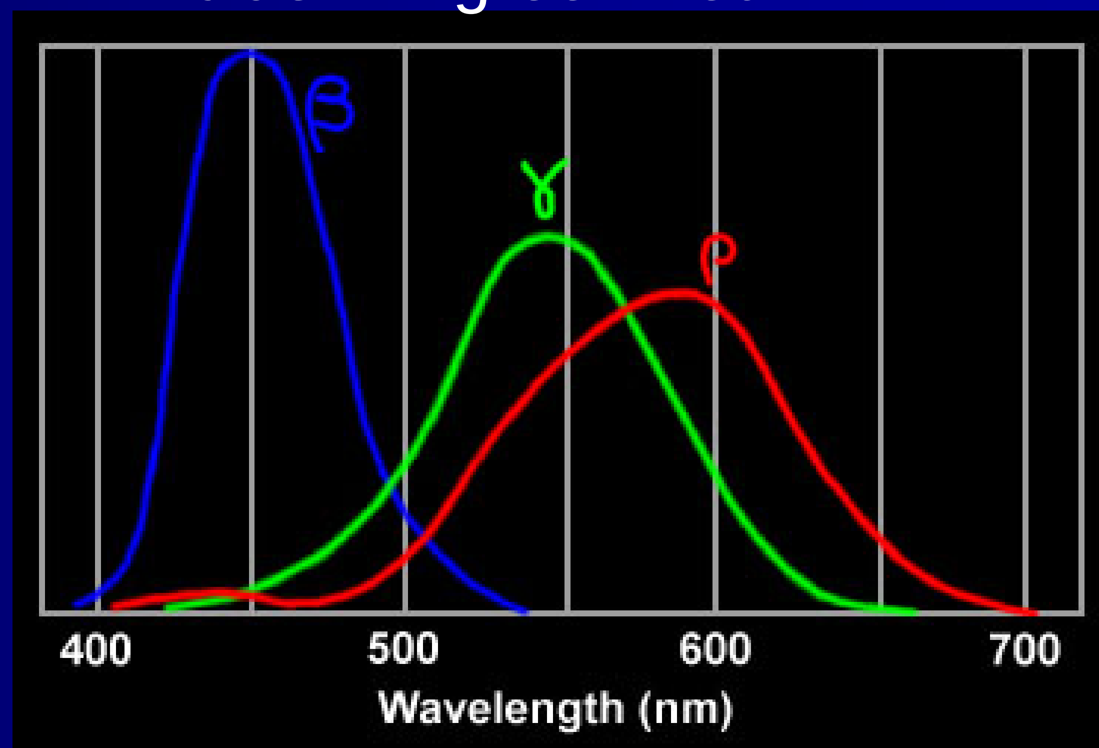

Rods do not see red:

- red rose at twilight;
- red instrument light of the ship captain

Geometry of rods

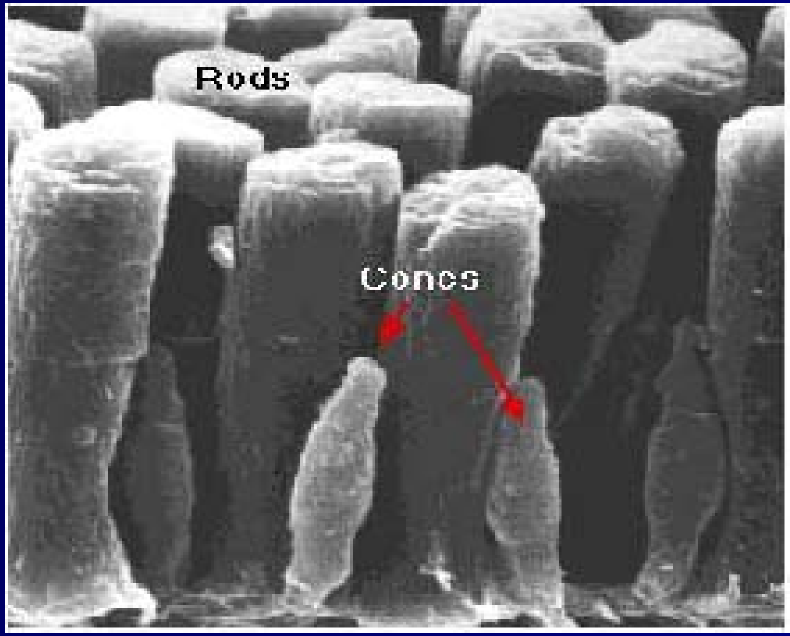

ROD (salamander):
height ≈ 20 μm
radius ≈ 3 μm

ROD (humans):
height ≈ 20 μm
radius ≈ 0.5 μm

Structure of rods

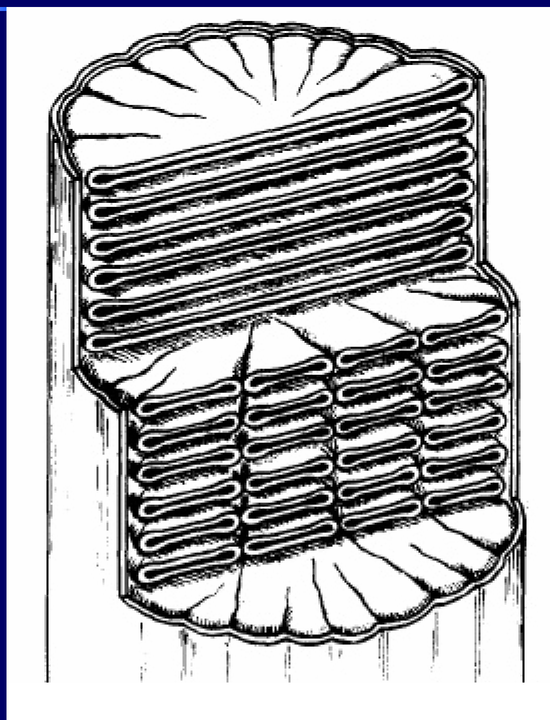

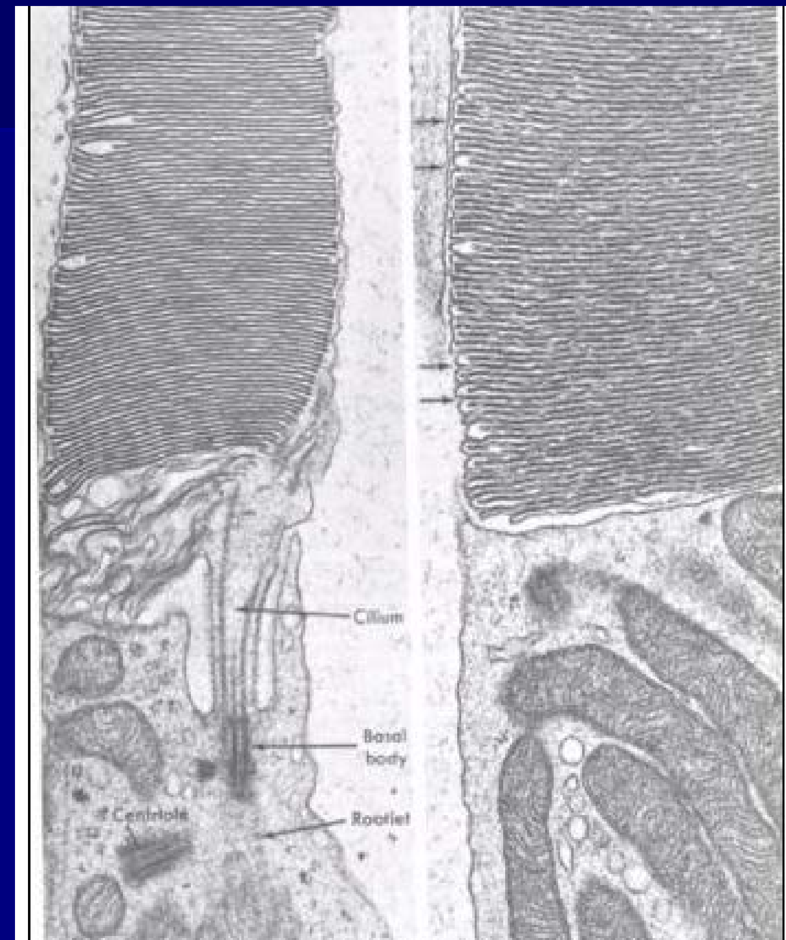

A thousand flattened sacs (“disks”) fill rod outer segment

Structure of rods

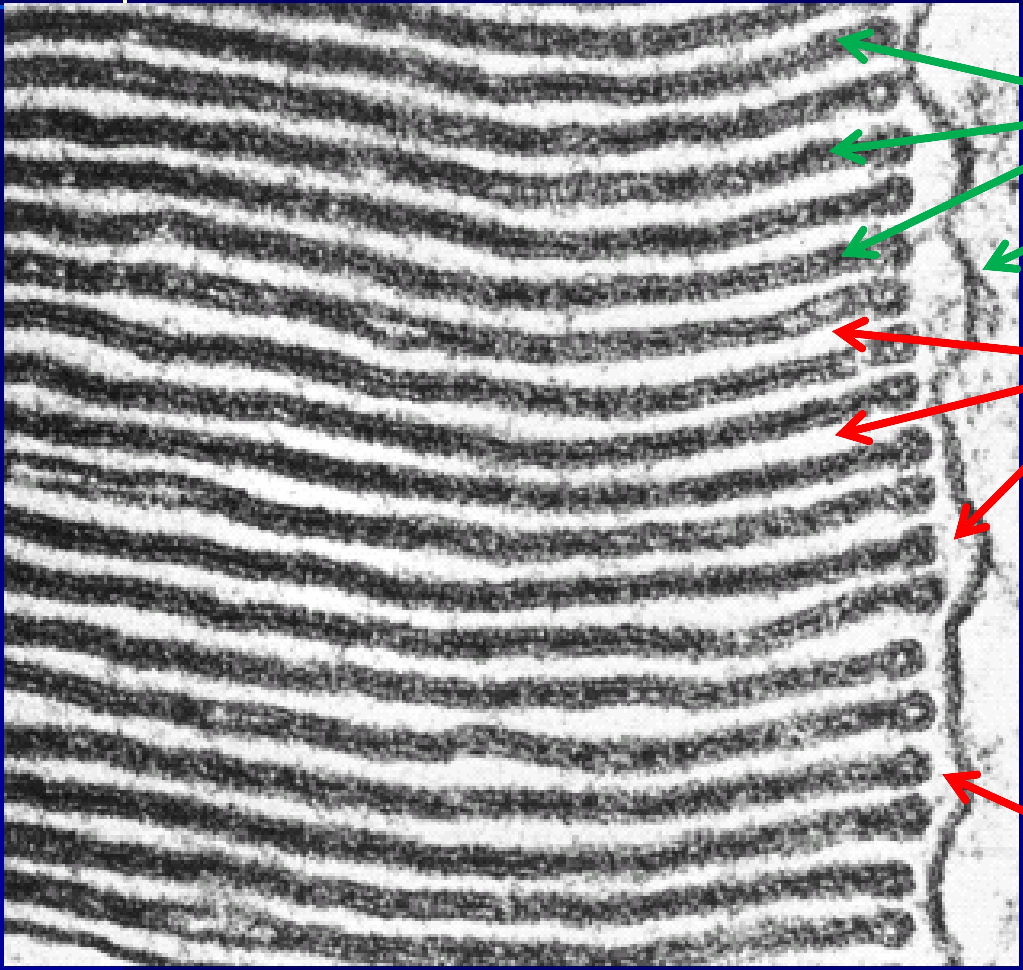

2D structures:
- Disc membranes
- Plasma membrane

3D structure: cytosol

discs ≈ 800
- width ≈ 15 nm
- distance ≈ 15 nm

outer shell thickness ≈ 15 nm

Phototransduction cascade

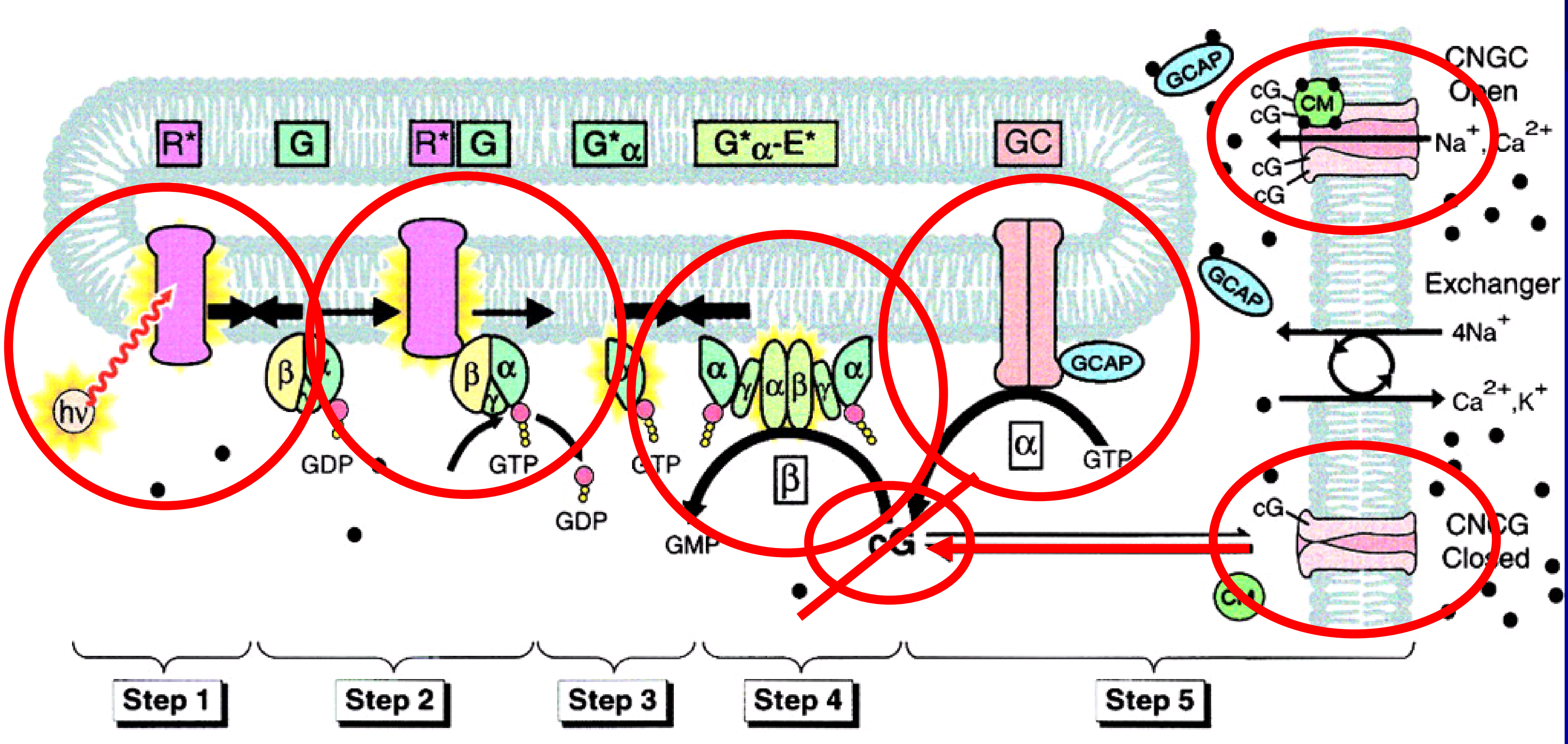

- Initial steps occur on the disk surface → cG depletion
- cG diffusion → CNGC close → Ca^{2+} depletion, elect. resp.

Bridging between scales: Nano to Micro

Biophysical phenomenon strongly depends on cell nanostructure

Biological output operates at cellular level

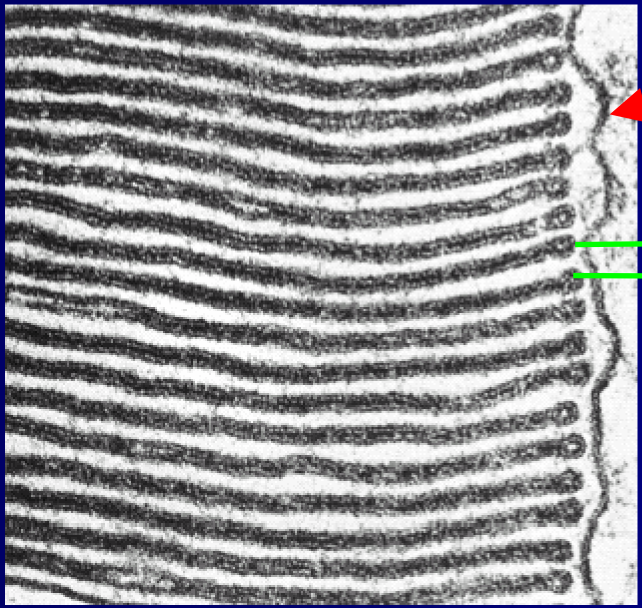

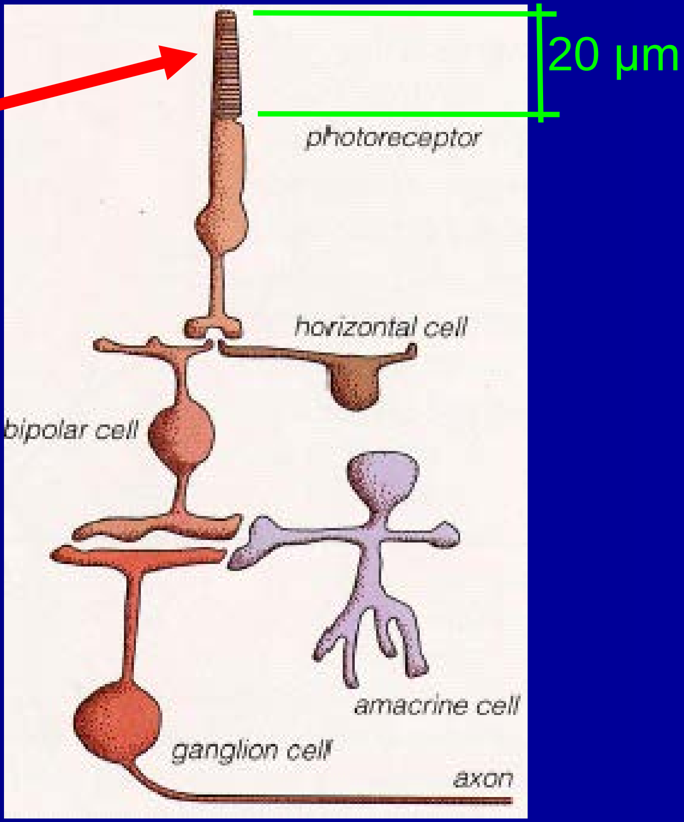

Homogenization

Nanoscale: diffusion equations

diffusion of cG (cyclic guanosine monophosphate)

$$\frac{\partial[\mathrm{cG}]}{\partial t} - D_{\mathrm{cG}}\nabla^2[\mathrm{cG}] = 0$$

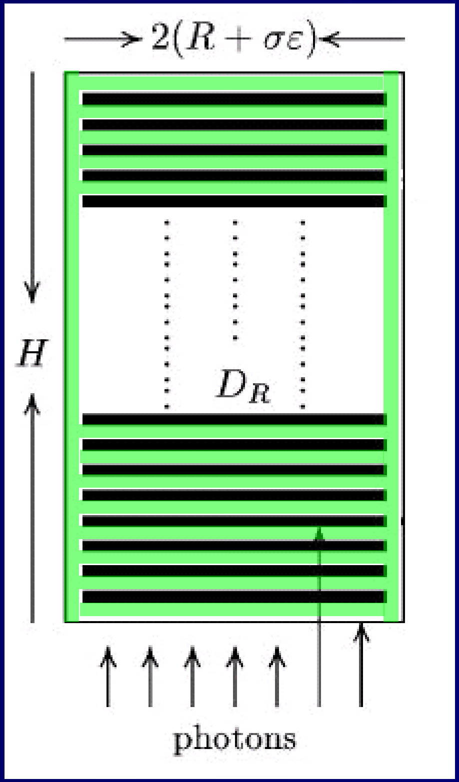

diffusion of Ca^{2+} (calcium ion)

$$\frac{\partial[\mathrm{Ca}^{2+}]}{\partial t} - D_{\mathrm{Ca}}\nabla^2[\mathrm{Ca}^{2+}] = 0$$

in the cytosol:
a perforated domain

Nonlinear boundary-flux terms

Membrane-bound enzymes acting on cytosolic substrates

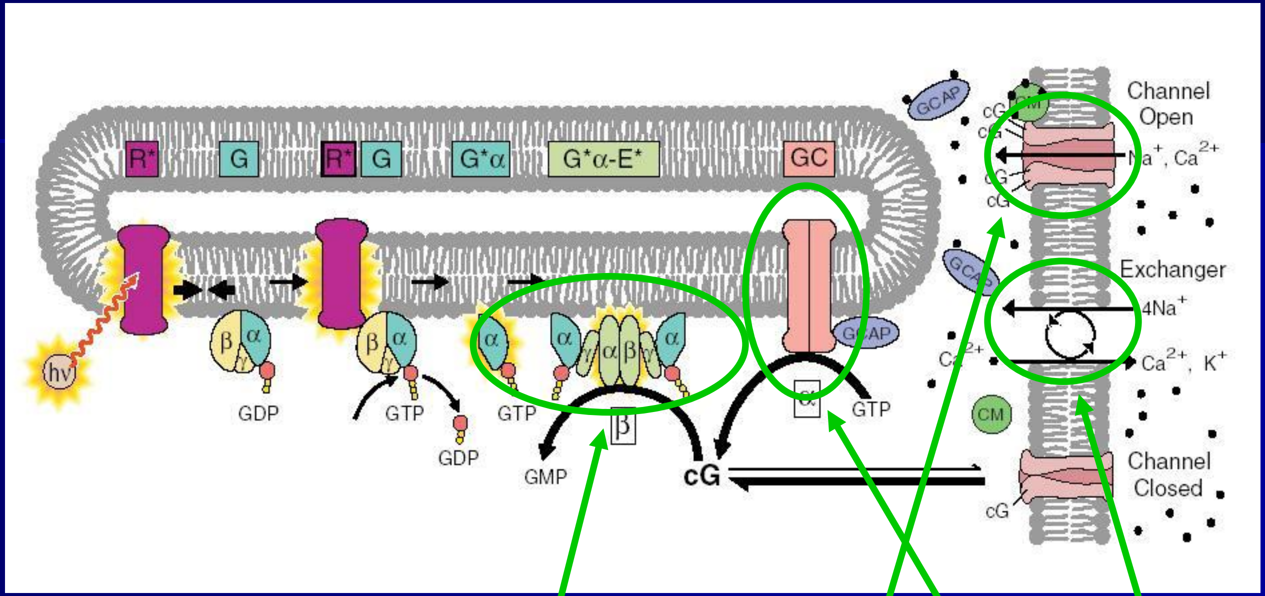

$$-D_{\mathrm{cG}}\nabla[\mathrm{cG}]\cdot n = E^*_\sigma[\mathrm{cG}] - \frac{\alpha}{1+([\mathrm{Ca}^{2+}]/\beta)^m}$$

Boundary flux terms on specific surfaces

Alleviating geometric complexity

Inner cylinder:

Periodic structure

Homogenization (period ε → 0)

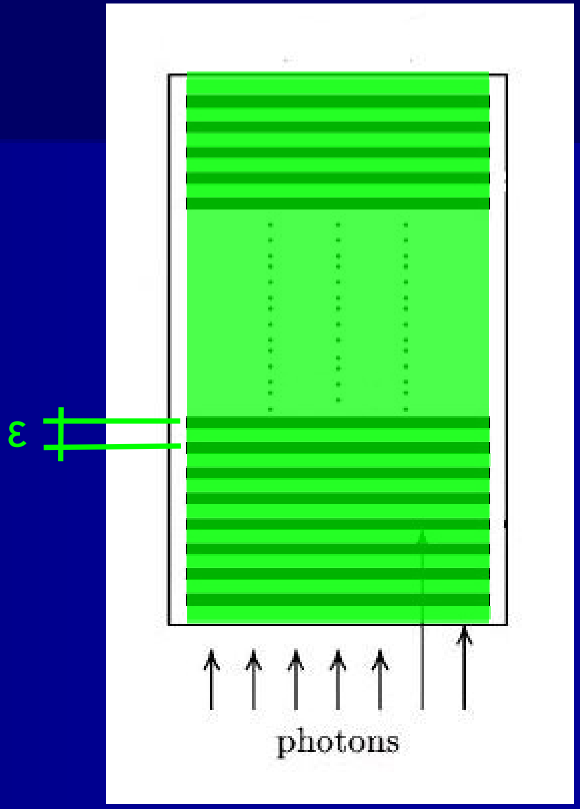

Perforated domain → Effective anisotropic medium

3D diffusion in interdiscal spaces → Family of 2D diffusion parametrized by the longitudinal variable z

Alleviating geometric complexity

Outer shell:

Thin layer

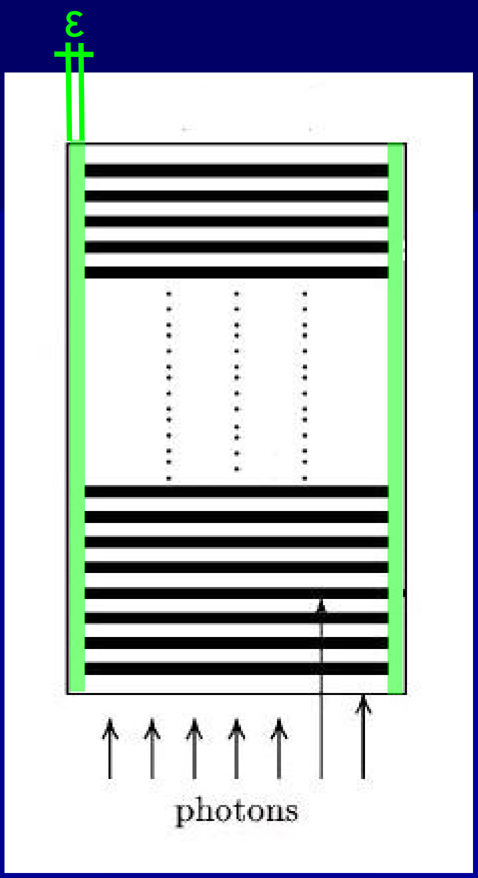

Concentrating capacity (thickness $\varepsilon \rightarrow 0$)

Mass conservation: rescale capacity and diffusion coefficients by $a_\varepsilon \approx 1/\varepsilon$

Outer shell diffusion (3D)

Surface diffusion (2D)

Limit as ε → 0

A-priori estimates (uniform w. r. to ε)

- Energy estimate (u_ε stands for [cG] or [Ca^{2+}]):

$$\sup_{0 \le t \le T} \left\| \sqrt{a_\varepsilon}\, u_\varepsilon(\cdot, t) \right\|_{2,\tilde{\Omega}_\varepsilon} + \left\| \sqrt{a_\varepsilon} \nabla u_\varepsilon \right\|_{2,\tilde{\Omega}_{\varepsilon,T}} \le \gamma$$

- Equiboundedness: $0 \le u_\varepsilon(x,t) \le \gamma$

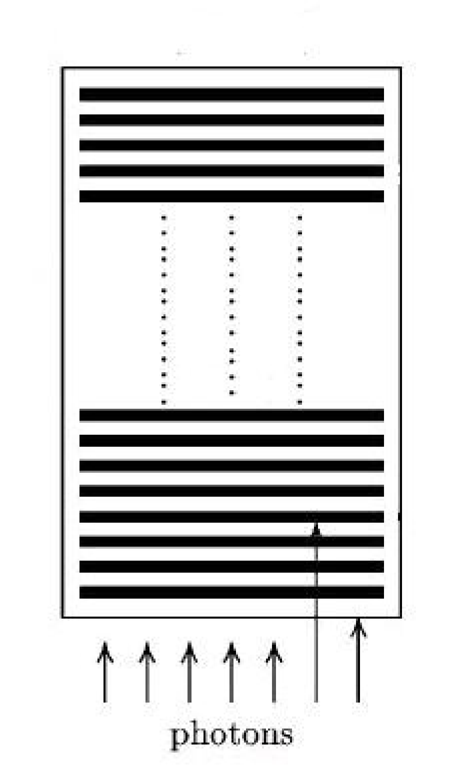

Perforated domain depends on ε

Need to extend u_ε inside the holes

(in Cioranescu, Saint Jean Paulin, 1998, homogeneous Neumann boundary conditions)

H^1 extension of u_ε

$\bar{u}_\varepsilon(P)$ inside a hole:

weighted mean of $u_\varepsilon(P_1)$ and $u_\varepsilon(P_2)$ at reflected points P_1 and P_2 inside adjacent interdiscal spaces

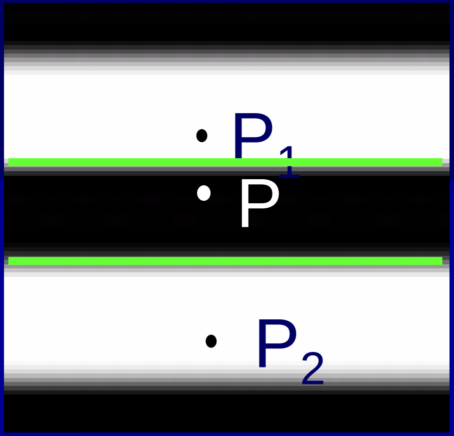

But $u_\varepsilon(P_1)$ and $u_\varepsilon(P_2)$ seem to be not related to each other:

Why should the extension $\bar{u}_\varepsilon$ have any uniform regularity in z?

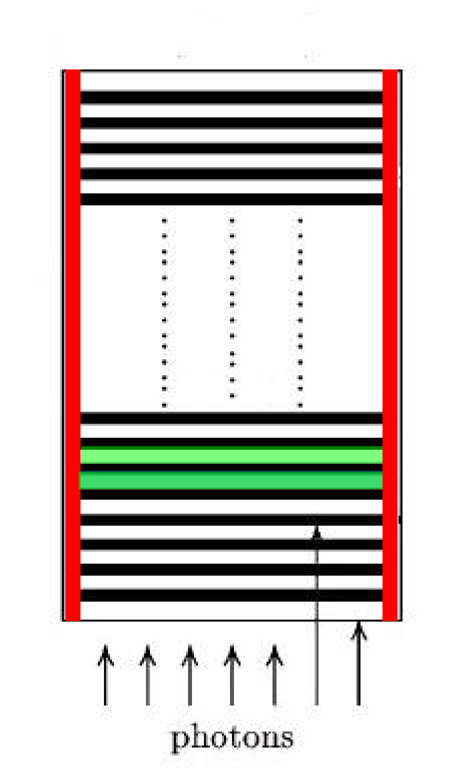

$$\left\| \overline{u}_\varepsilon(z+h) - \overline{u}_\varepsilon(z) \right\|_{2,\Omega_{o,T}} \leq \gamma h$$

$$\left\| \overline{u}_\varepsilon \right\|_{L^2(0,T;W^{1,2}(\Omega_o))} \leq \gamma$$

Almost disconnected structures

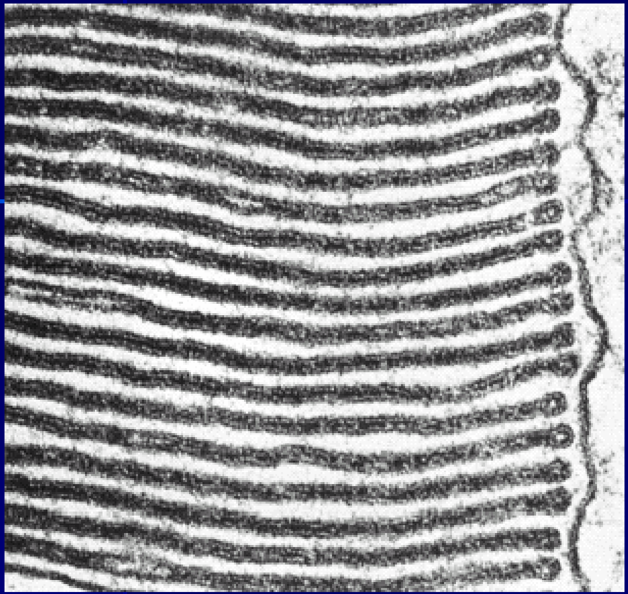

Bladed rotors

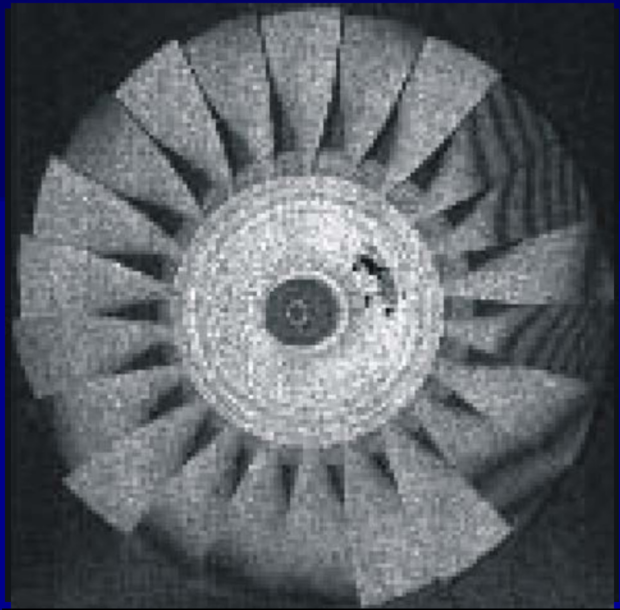

Vibration localization

Homogenization

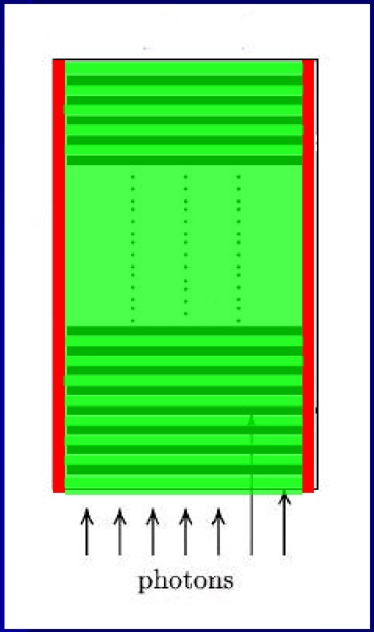

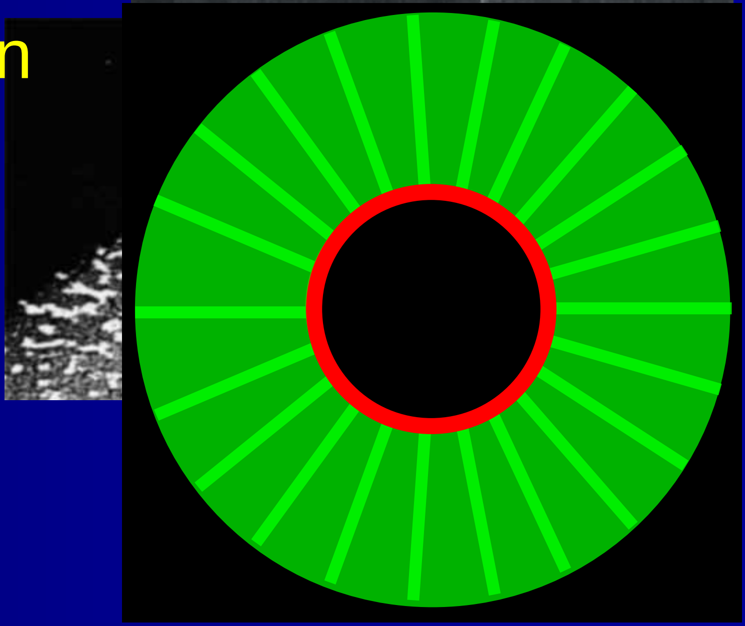

Phototransduction

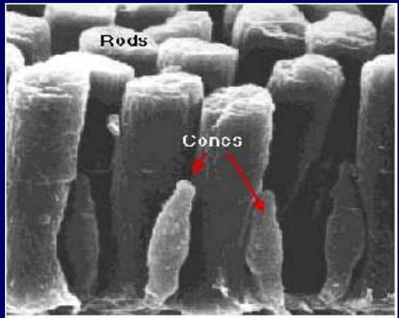

Model at microscale

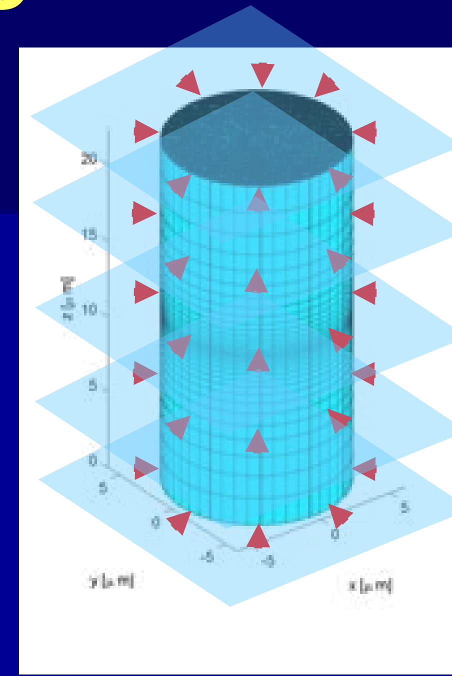

- Interior limit (u): family of 2D diffusions driven by volumic source f accounting for flux on discs

$$u_t - \Delta_{\overline{x}} u = -(u - f)$$

- Limit on the outer shell ($\hat{u}$):

$$\hat{u}(\theta, z, t) = u(\overline{x}, z, t)\Big|_{|\overline{x}|=R}$$

2D diffusion driven by outflux from interior

$$\hat{u}_t - \Delta_S \hat{u} = -\frac{(1-\theta_o)}{\sigma \varepsilon_o} u_\rho \Big|_{|\overline{x}|=R} + g$$

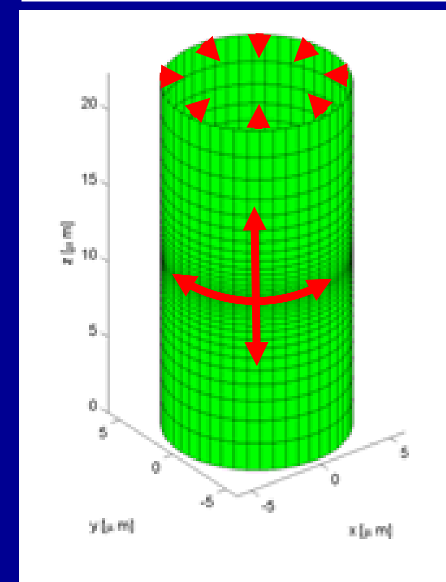

Reduced model

ROD (humans)

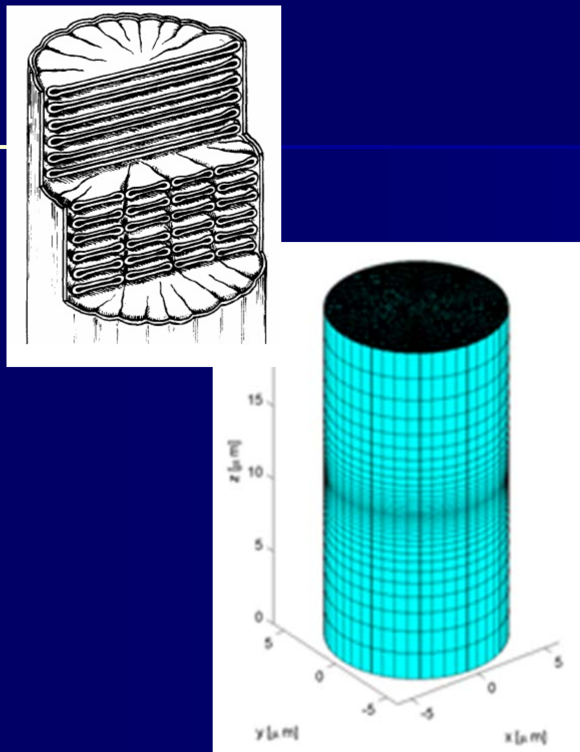

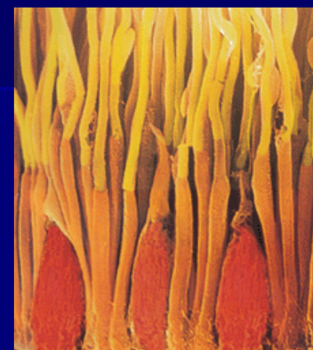

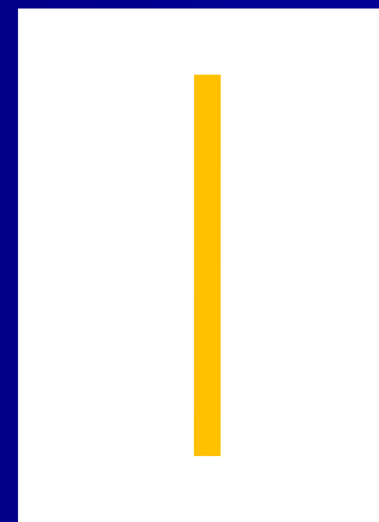

Family of 2D diffusions
+ diffusion on outer shell

1D diffusion:

$$\frac{\partial[\mathrm{cG}]}{\partial t} - D_{\mathrm{eff}}\frac{\partial[\mathrm{cG}]}{\partial z^2} = -\beta[\mathrm{cG}] + f([\mathrm{Ca}^{2+}])$$

Example: variability of the response

Observed

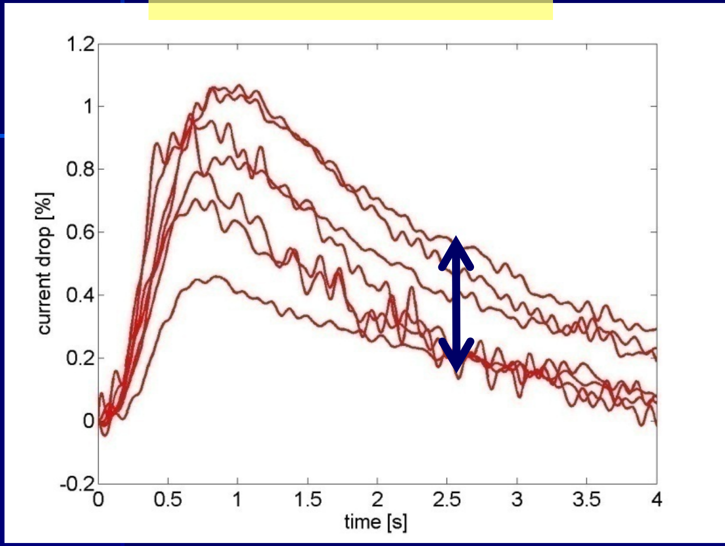

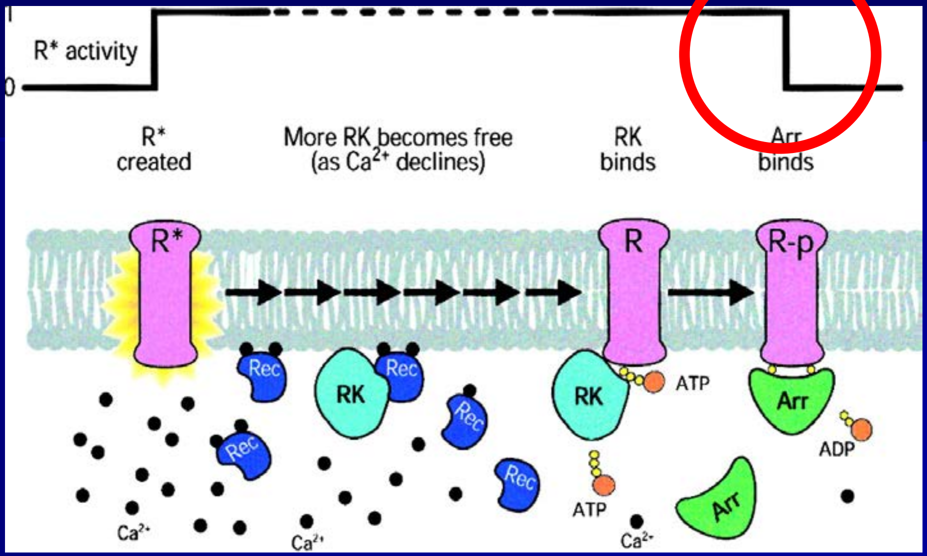

Expected, based on R* decay time

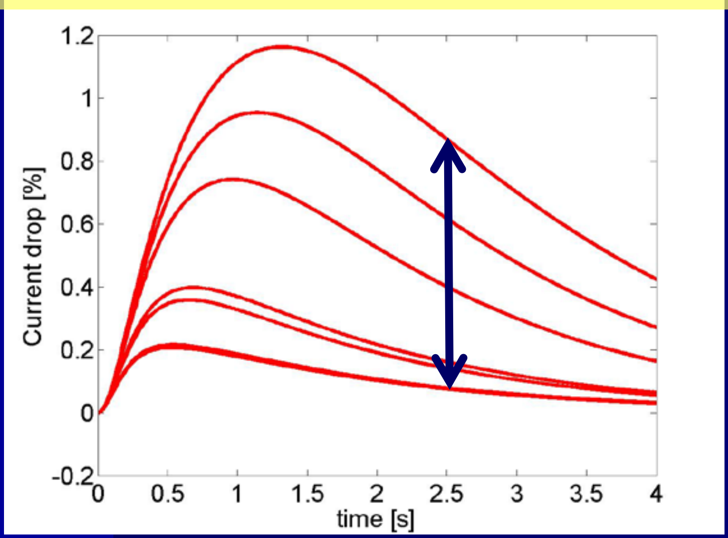

Variability is mainly due to randomness of R* shutoff

Observed variability is lower than expected

Model quantitatively accounts for variability reduction: Diffusion / “Cellar effect”

Perspectives

- Spatio-temporal model: useful to tackle open biophysical problems (e.g., light adaptation, cones)
- Similar approach to model other signaling networks

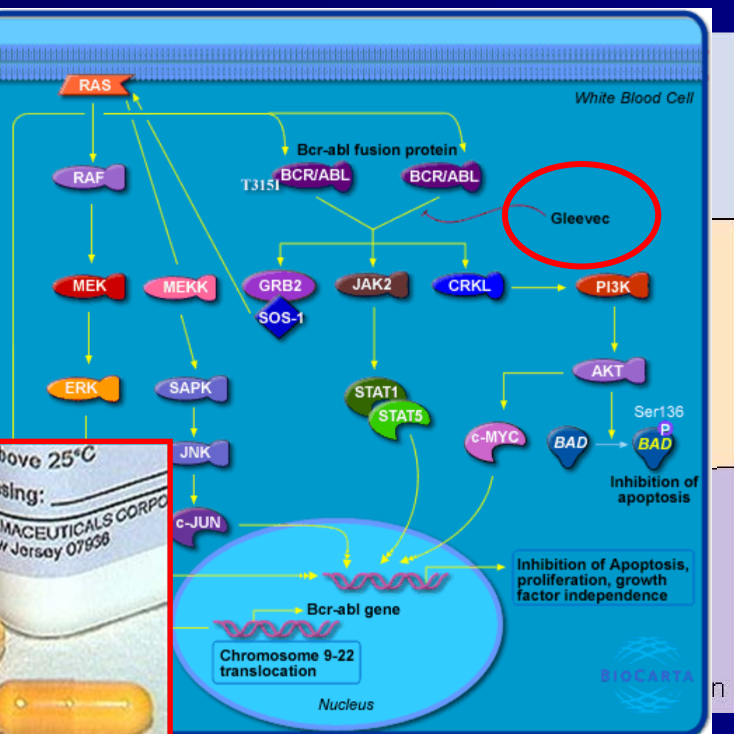

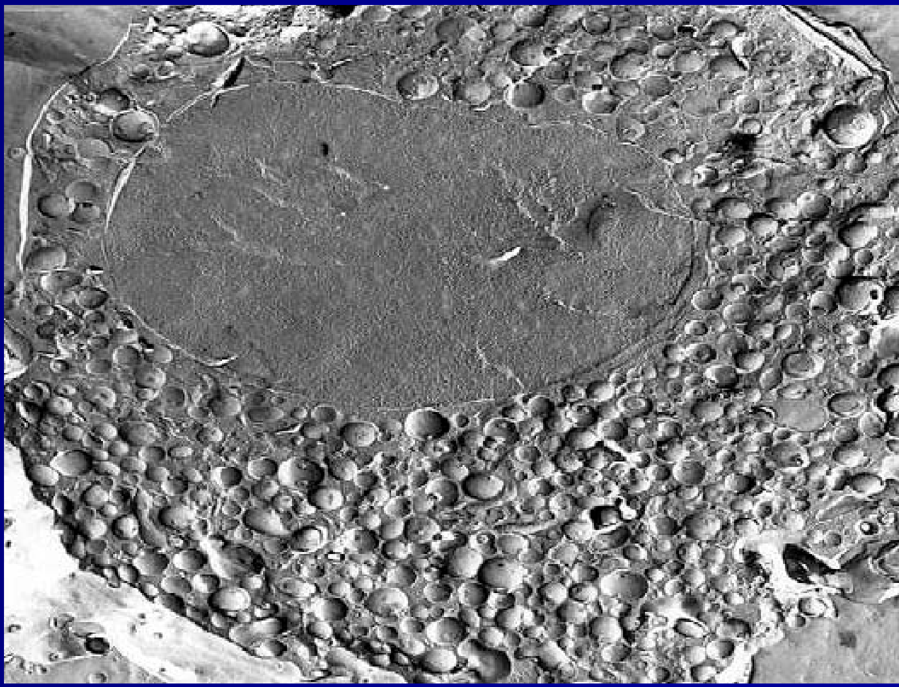

Bioimpedance measurements

Non-invasive diagnosis and treatment

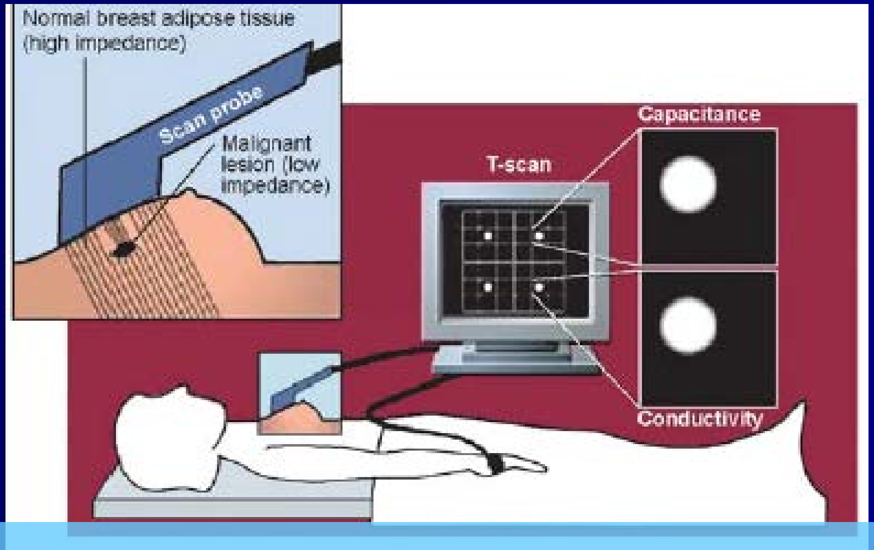

Electrical Impedance Tomography

Monitoring of transplant organs

Virtual biopsy, RF-ablation, dialysis

Measurements currently fitted by phenomenological models: ambiguities arise

Aim: to determine the relationships between effective dielectric properties and properties of the constituents

Electric conduction

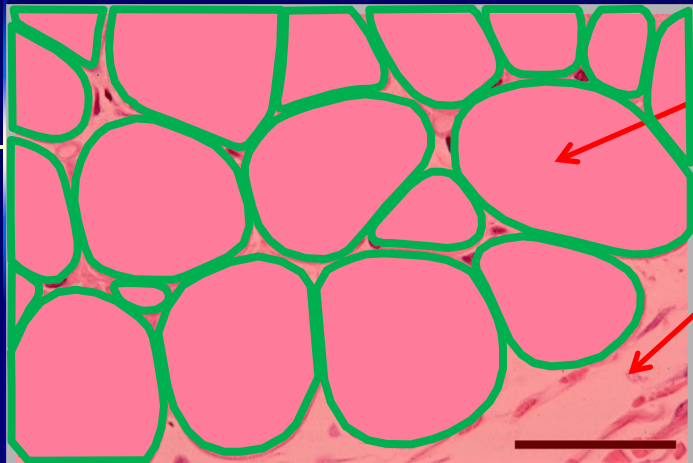

Intra-/extra- cellular space

$$\mathrm{div}(\sigma \nabla w_\varepsilon) = 0$$

w_ε: electric potential

σ : conductivity

ε : microstructural scale

Capacitive-conductive behavior:

Imperfect interface

$$[\![\sigma \nabla w_\varepsilon \cdot \nu]\!] = 0$$

$$\frac{\epsilon_o \epsilon_r}{\varepsilon d} \frac{\partial [\![w_\varepsilon]\!]}{\partial t} + \frac{\sigma}{\varepsilon d} [\![w_\varepsilon]\!] = \sigma \nabla w_\varepsilon \cdot \nu$$

Cell

$[\![w_\varepsilon]\!]$

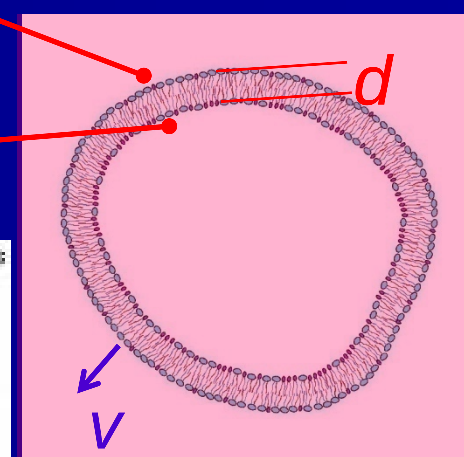

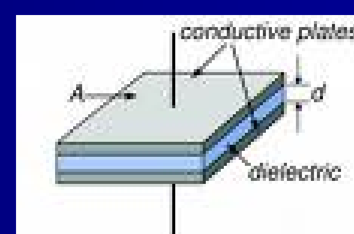

Anti-plane problem

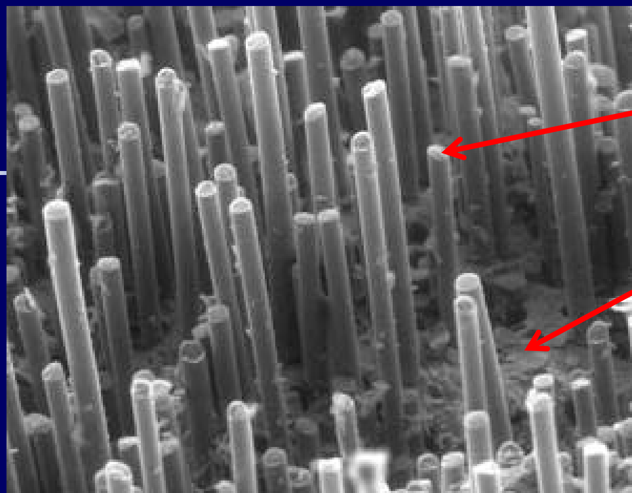

Fibre / matrix

$$\mathrm{div}(G\nabla w_\varepsilon) = 0$$

w_ε: longitudinal displacement

G : shear modulus

ε: microstructural scale

Imperfect interface

Lene & Leguillon, 1981; Hashin, 1991; Bigoni et al., 1998

Kelvin-Voigt model

Interface

$$[\![w_\varepsilon]\!]$$

$$[\![G\nabla w_\varepsilon \cdot \nu]\!] = 0$$

$$\frac{\eta}{\varepsilon d}\frac{\partial [\![w_\varepsilon]\!]}{\partial t} + \frac{E}{\varepsilon d}[\![w_\varepsilon]\!] = G\nabla w_\varepsilon \cdot \nu$$

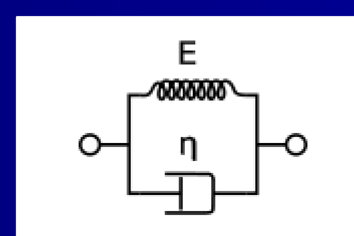

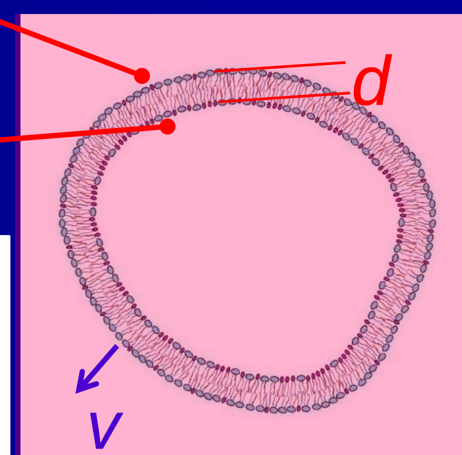

Bridging between scales: Micro to Macro

Biophysical phenomenon strongly depends on tissue microstructure

Measurements are taken at organ level

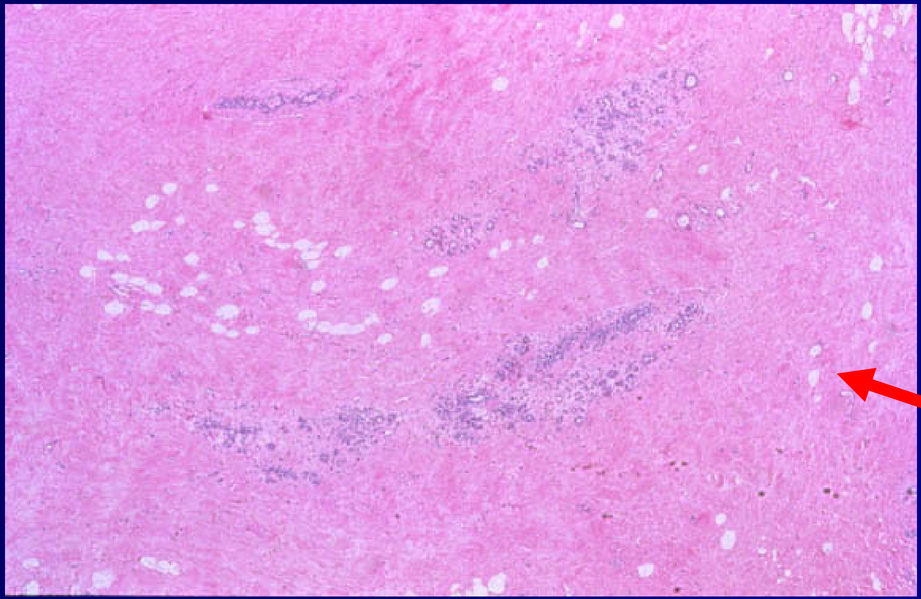

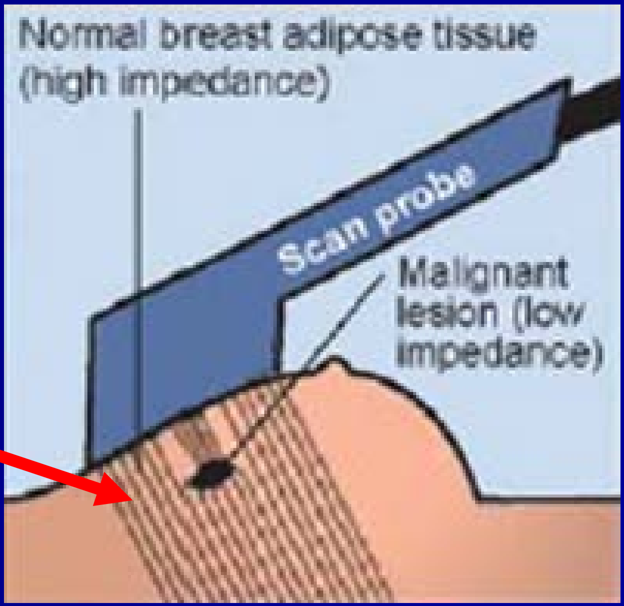

Homogenization

Limit as ε → 0

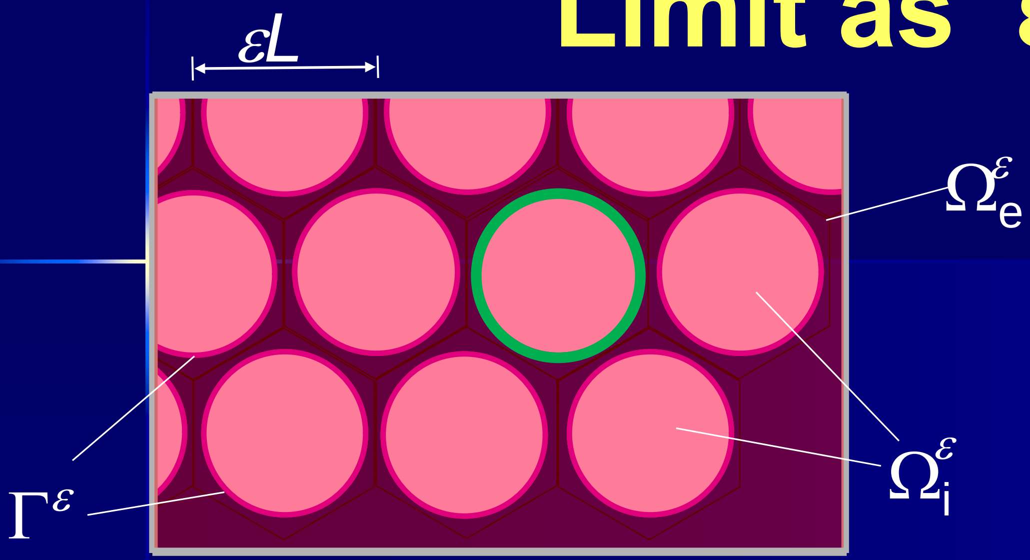

Periodic microstructure

$$w_\varepsilon \in H^1(\Omega_i^\varepsilon) \cap H^1(\Omega_e^\varepsilon)$$

$$\boxed{w_\varepsilon \notin H^1(\Omega)}$$

Energy estimate:

$$\int_0^t \int_\Omega \sigma |\nabla w_\varepsilon|^2 \, \mathrm{d}x \, \mathrm{d}t + \frac{1}{\varepsilon} \int_{\Gamma^\varepsilon} [\![w_\varepsilon]\!]^2 (x,t) \, \mathrm{d}\sigma \le \gamma$$

Poincare's inequality (Hom. Dirichlet b.c. on $\partial\Omega$):

$$\int_\Omega v^2 \, \mathrm{d}x \le C \left\{ \int_\Omega |\nabla v|^2 \, \mathrm{d}x + \frac{1}{\varepsilon} \int_{\Gamma^\varepsilon} [\![v]\!]^2 \, \mathrm{d}\sigma \right\}$$

Equiboundedness in $H^s(\Omega)$, $0<s<½$ → strong L^2 conv.

(Hummel, 1999)

Limiting equation

$w_\varepsilon \longrightarrow w_o$ $\sigma \nabla w_\varepsilon \rightharpoonup \xi$ $\mathrm{div}\xi = 0$

How are w_o and $\boldsymbol{\xi}$ related to each other ?
What is the effective constitutive equation ?

Oscillating test function method (Tartar, 1977)
(→ imperfect interfaces & time-dependent behavior)

$$\xi = \sigma^{\#} \nabla w_0 + \int_0^t F(t-\tau) \nabla w_0(x,\tau)\, \mathrm{d}\tau + \mathcal{S}$$

Memory effects appear

Barbero et al, 1995
Yeong-Moo et al., 1998
Giorgi et al., 2001
Friebel et al., 2006
Appleby et al., 2006

Effective behavior

Fourier transform in time & asymptotic expansion:

$$w_\varepsilon = w_0(x) - \varepsilon \boldsymbol{\chi}(y) \cdot \nabla w_0(x) + \ \ldots$$

Cell-problem

$$\begin{aligned} -\sigma \Delta_y \chi_h &= 0 && \text{in } Q_\mathrm{i} \cup Q_\mathrm{e} \\ [\![\sigma(\nabla_y \chi_h - \mathbf{e}_h) \cdot \nu]\!] &= 0 && \text{on } \Gamma \\ Y[\![\chi_h]\!] = \sigma(\nabla_y \chi_h - \mathbf{e}_h) \cdot \nu && && \text{on } \Gamma \end{aligned}$$

Lord Rayleigh, 1892
Gu et al, 1992
Nicorovici et al, 1993
Sangani et al, 1997
Cheng et al, 1997
Rodrìguez-Ramos, 2001
Jiang at al, 2004

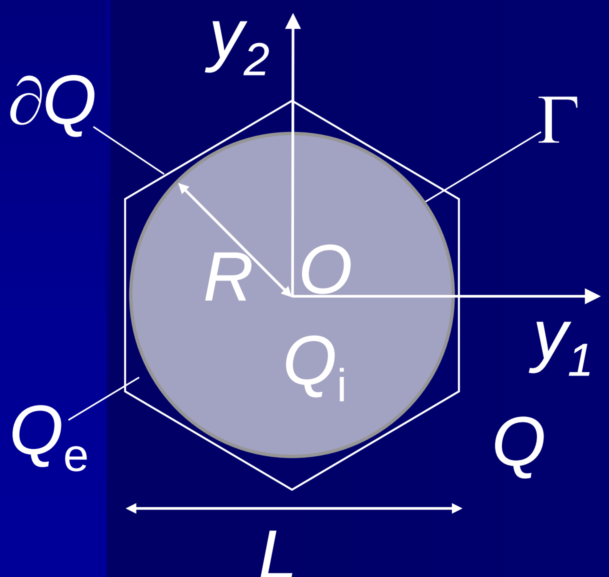

Solution (Fourier series in space)

$$\chi_\mathrm{i} = \sum_{m=1}^{+\infty}{}^{\circ} \, a_m \left(\frac{r}{R}\right)^m \cos m\theta$$

$$\chi_\mathrm{e} = \sum_{m=1}^{+\infty}{}^{\circ} \left[b_m \left(\frac{r}{R}\right)^m + b_{-m} \left(\frac{r}{R}\right)^{-m} \right] \cos m\theta$$

$$\chi_\mathrm{e} = -c_1 \Re\left(\frac{\eta_1}{\omega_1} z\right) + \sum_{s=1}^{+\infty}{}^{\circ} \, c_s \Re\left(\frac{\zeta^{(s-1)}(z)}{(s-1)!}\right)$$

Effective behavior

Closed-form effective conductivity (Fourier domain)

$$\frac{\sigma^{\#}}{\sigma_{\mathrm{e}}} = \frac{\gamma_1^- \sum_{n=0}^{N} \sum_{I \in_N \mathcal{C}_n} (\det M_{I,I}) \prod_{k \in I} (\gamma_k^-)^{-1} \left(\frac{\omega_1}{\eta_1} f \right)^{|I|}}{\gamma_1^+ \sum_{n=0}^{N} \sum_{I \in_N \mathcal{C}_n} (\det M_{I,I}) \prod_{k \in I} (\gamma_k^+)^{-1} \left(\frac{\omega_1}{\eta_1} f \right)^{|I|}}$$

f : volume fraction; γ's : material parameters; others : geometry

Truncation order *N*=4

$$\frac{\sigma^{\#}}{\sigma_{\mathrm{e}}} = 1 - \frac{2f}{\gamma_1} \left[1 + \frac{f}{\gamma_1} - \frac{\frac{p_{1,5} f^6}{\gamma_1 \gamma_5}}{1 - \frac{p_{5,7} f^{12}}{\gamma_5 \gamma_7}} \right]^{-1}$$

Perspectives

Extension to nonperiodic structures

Applications: Virtual biopsy, RF-ablation, monitoring cell growth and adhesion, device optimization

Modeling electroporation: gene therapy, bioavailability of drugs (electrochemotherapy)